The PET Radioligand ^{18}F-FIMX Images and Quantifies Metabotropic Glutamate Receptor 1 in Proportion to the Regional Density of Its Gene Transcript in Human Brain

Paolo Zanotti-Fregonara[1,2], Rong Xu[1], Sami S. Zoghbi[1], Jeih-San Liow[1], Masahiro Fujita[1], Mattia Veronese[3], Robert L. Gladding[1], Denise Rallis-Frutos[1], Jinsoo Hong[1], Victor W. Pike[1], and Robert B. Innis[1]

[1]Molecular Imaging Branch, National Institute of Mental Health, Bethesda, Maryland; [2]INCIA UMR-CNRS 5287, University of Bordeaux, Bordeaux, France; and [3]Department of Neuroimaging, IoPPN, King's College London, London, United Kingdom

A recent study from our laboratory found that ^{18}F-FIMX is an excellent PET radioligand for quantifying metabotropic glutamate receptor 1 (mGluR1) in monkey brain. This study evaluated the ability of ^{18}F-FIMX to quantify mGluR1 in humans. A second goal was to use the relative density of mGluR1 gene transcripts in brain regions to estimate specific uptake and nondisplaceable uptake (V_{ND}) in each brain region. **Methods:** After injection of 189 ± 3 MBq of ^{18}F-FIMX, 12 healthy volunteers underwent a dynamic PET scan over 120 min. For 6 volunteers, images were acquired until 210 min. A metabolite-corrected arterial input function was measured from the radial artery. Four other subjects underwent whole-body scanning to estimate radiation exposure. **Results:** ^{18}F-FIMX uptake into the human brain was high (SUV = 4–6 in the cerebellum), peaked at about 10 min, and washed out rapidly. An unconstrained 2-tissue-compartment model fitted the data well, and distribution volume (V_T) (mL·cm^{-3}) values ranged from 1.5 in the caudate to 11 in the cerebellum. A 120-min scan provided stable V_T values in all regions except the cerebellum, for which an acquisition time of at least 170 min was necessary. V_T values in brain regions correlated well with mGluR1 transcript density, and the correlation suggested that V_{ND} of ^{18}F-FIMX was quite low (0.5 mL·cm^{-3}). This measure of V_{ND} in humans was similar to that from a receptor blocking study in monkeys, after correcting for differences in plasma protein binding. Similar to other ^{18}F-labeled ligands, the effective dose was about 23 μSv/MBq. **Conclusion:** ^{18}F-FIMX can quantify mGluR1 in the human brain with a 120- to 170-min scan. Correlation of brain uptake with the relative density of mGluR1 transcript allows specific receptor binding of a radioligand to be quantified without injecting pharmacologic doses of a blocking agent.

Key Words: mGluR1; ^{18}F-FIMX; PET; gene transcripts

A PET radioligand for metabotropic glutamate receptor 1 (mGluR1) would be useful for exploring the potential role of this receptor in the pathophysiology of neuropsychiatric disorders and to facilitate the development of novel therapeutic drugs. However,

design of PET radioligands for mGluR1 is challenging. Among the numerous demanding criteria that a prospective radioligand must fulfill (*1*), high affinity and selectivity are particularly difficult to achieve for mGluR1 imaging agents. In fact, mGluR1 belongs to the same family subgroup as mGluR5 and has a similar structure, DNA sequence, and function. Therefore, ligands engineered to bind to mGluR1 tend to cross-react with mGluR5. Indeed, several mGluR1 radioligands have been reported in the literature (*2*), but most were stopped at the preclinical level because of some unfavorable imaging characteristics.

To date, only 2 mGluR1 PET radioligands have been evaluated in humans. The first, the isothiazole derivative mGluR1 antagonist ^{11}C-LY2428703, showed good characteristics both in vitro and in vivo in rats (*3*). It was, however, unsuitable for both monkey and human imaging because of low brain uptake, which was possibly caused by high binding to plasma proteins (*4*). The second, ^{11}C-ITMM, was also successfully validated in rodents (*5*). Disadvantages in humans, however, included an overall low brain uptake and slow uptake and washout; as a result, ^{11}C-ITMM is unlikely to quantify mGluR1 within the time constraints of the half-life (20 min) of ^{11}C (*6*).

We recently developed a novel mGluR1 radioligand, ^{18}F-FIMX, which has excellent imaging characteristics based on in vitro properties and in vivo imaging in monkey brain. ^{18}F-FIMX has high affinity (half maximal inhibitory concentration, 5.1 nM) for human mGluR1, relatively low affinity for mGluR5 (8 μM (*7*)), suitable lipophilicity (LogD = 2.5), and a high ratio of specific (V_S) to nondisplaceable uptake (V_{ND}) in monkey brain (*8*). Thus, one aim of this study was to evaluate the ability of ^{18}F-FIMX to quantify mGluR1 in the human brain.

An important performance characteristic of any radioligand is its ratio of signal to noise—more specifically, its ratio of V_S to V_{ND}. In the absence of any receptor-free region, measuring this ratio typically requires administering pharmacologic doses of a blocking agent that often does not exist for human use, especially for novel targets. For drug doses that do not completely block all receptors, the Lassen plot (*9*) uses a simple regression of V_S to total distribution volume (V_T) to estimate V_{ND}; this assumes that V_{ND} is the same in all brain regions, which is almost always the case.

This paper explored whether the relative regional density of mGluR1 gene transcript could be used as a substitute for V_S, thereby allowing V_{ND} to be estimated without injecting any blocking drug. The rationale for this approach is that many gene transcripts are linearly related to the expression of the protein—that is, linearly proportional to the density of the receptor (*10*). For any given protein target, one must first confirm that the gene transcript (messenger

RNA [mRNA]) is linearly proportional with protein density. Thus, we first explored whether mGluR1 gene transcript is proportional to receptor density measured with PET and then used this linear correlation to estimate the V_{ND} of ^{18}F-FIMX. This allowed V_S and the ratio of V_S to V_{ND} to be calculated in each brain region. Furthermore, because the relative density of about 30,000 gene transcripts in regions of the human brain are now available in the Allen Brain Atlas (11), this method is potentially useful for numerous other PET imaging targets to estimate V_S to V_{ND} of the associated radioligand. Thus, the 2 aims of this paper were to evaluate the ability of ^{18}F-FIMX to quantify mGluR1 in the human brain and to explore whether the relative density of mGluR1 gene transcript could be used to estimate the ratio of V_S to V_{ND} of the radioligand. In addition, because V_{ND} is typically similar across species, we validated the estimations in humans by calculating the V_{ND} of ^{18}F-FIMX in a monkey after complete receptor blockade.

MATERIALS AND METHODS

Radioligand Preparation

^{18}F-FIMX was produced from ^{18}F-fluoride ion and an N-Boc–protected (phenyl)aryliodionium salt precursor as previously described (8). The radioligand was prepared according to our investigational new drug application (#119,521), available at http://pdsp.med.unc.edu/snidd/. The radioligand was obtained with high radiochemical purity (>99%) and specific activity at the time of injection of 61.8 ± 36.7 GBq/μmol. The mass dose was 0.09 ± 0.12 nmol/kg (range, 0.02–0.46 [n = 16]).

Subjects

Twelve healthy subjects (4 men, 8 women; age ± SD, 28 ± 10 y; weight ± SD, 73 ± 15 kg) underwent a brain scan, and an additional 4 subjects (2 men, 2 women; age ± SD, 31 ± 14 y; weight ± SD, 62 ± 8 kg) underwent a whole-body scan. All subjects were free of medical and neuropsychiatric diseases, as determined by medical history, physical examination, electrocardiogram, and laboratory blood and urine tests. Vital signs were monitored before ligand injection and then during and after completion of the scan. Urinalysis and blood lab tests were repeated within a few hours of completion of the PET scan. The study was approved by the Institutional Review Board, and all subjects signed a written informed consent form.

Plasma Measurements

After radioligand injection, arterial blood samples (1.5 mL each) were drawn from the radial artery at 15-s intervals until 120 s, followed by 3- to 5-mL samples at 3, 5, 10, 15, 20, 30, 45, 60, 75, 90, 105, and 120 min. For the 6 subjects who underwent a longer scan, additional samples were drawn at 135, 150, 165, 180, 195, and 210 min. The whole blood was first centrifuged to separate plasma. The concentration of parent radioligand in plasma was then measured by high-performance liquid chromatography in each blood sample (some blood samples around the peak of the input function, when the parent concentration is almost 100%, were interpolated) (12). All plasma input functions (and whole-blood curves) were well fitted by a triexponential function with gaussian weighting and used for kinetic modeling. The plasma free fraction (f_P) was measured by ultrafiltration (13).

Image Acquisition and Analysis

Image acquisition and analysis are presented in the supplemental data (available at http://jnm.snmjournals.org).

Quantification of ^{18}F-FIMX Binding

V_T was calculated using both compartmental and noncompartmental models. Noncompartmental models included the Logan graphical analysis (14), Ichise's multilinear analysis MA1 (15) and MA2 (15), Zhou's relative-equilibrium Gjedde–Patlak bi-graphical analysis (RE-GP) (16),

standard spectral analysis (SA) (17), and rank-shaping SA (RSSA) (18). Analyses were performed at the region and the voxel level (supplemental data). We also tested the possibility of obtaining measures of ^{18}F-FIMX binding noninvasively, by replacing the arterial input function with a pseudoreference region. ^{18}F-FIMX binding was thus calculated using a simplified reference tissue model (SRTM), an SUVR, and brain uptake itself (SUV) (supplemental data).

mGluR1 Transcript as Surrogate of Receptor Density

mRNA transcription maps were obtained from the 6 donors of the Allen Human Brain Atlas (http://human.brain-map.org/) (11). Three probes related to the expression of mGluR1 were available for each donor: A_23_P30976 (probe A), CUST_14602_PI416261804 (probe B), and CUST_320_PI416408490 (probe C). Regional mRNA values were obtained by averaging the individual samples of each region (i.e., the coarse resolution of the Atlas), expressed in log2 scale. Because mRNA was sampled from both the caudate and the putamen for all donors, values in the striatum were compared with the average of the caudate and putamen on PET. Similarly, mRNA values in the cingulum were compared with the average of anterior and posterior cingulum on the PET images. Both mRNA and V_T values were preanalyzed with an autocorrelation analysis. As described by Rizzo et al. (10), the purpose of the autocorrelation analysis was to estimate data consistency with respect to intrasubject and intersubject variability. We first performed a Pearson analysis for each probe among the different donors, covering all possible combinations, to assess whether the values from different subjects were correlated and could thus be averaged to obtain 3 sequences of mRNA values corresponding to the 3 probes. We then performed the same autocorrelation among the 3 probes to select a representative one. The third autocorrelation was performed among the PET 2-tissue-compartment model V_T values of the different subjects to assess whether these data could be averaged to obtain regionwise representative values of ^{18}F-FIMX binding. Finally, the mRNA expression values of the representative probe were correlated to the averaged 2-tissue-compartment model/V_T values of ^{18}F-FIMX.

Estimation of V_{ND} of ^{18}F-FIMX Using mGluR1 Transcript Density

We postulated that mRNA expression would be proportional to V_S, mGluR1 would not be subject to significant posttranscriptional changes in vivo, and V_{ND} would be constant among the different brain regions. The mRNA values, expressed as log2 in the Allen Atlas, were first linearized and then linearly regressed against the 2-tissue-compartment model/V_T values obtained with the 120-min scans (for the cerebellum, the average of the value at 210 min [n = 6] was used, because it is more stable). Following the Lassen plot method (9,19), the x-axis intercept is equal to V_{ND}. V_{ND} estimated in humans was compared with that measured in a monkey after pharmacologic blockade (supplemental data).

Whole-Body Imaging and Dosimetry

Whole-body imaging and dosimetry are presented in the supplemental data.

Statistical Analysis

Goodness-of-fit by nonlinear least-squares analysis was evaluated using the Akaike information criterion, model selection criterion, and F statistics (20). P values of less than 0.05 were considered significant. The precision of the estimates was expressed as a percentage and equaled the ratio of the SE divided by the value itself. The SE was obtained from the diagonal of the covariance matrix (21) using the generalized form of the error propagation equation (22). Smaller values indicate higher precision. V_T values obtained using the different techniques, both at the regional and at the voxel level, were compared with the reference 2-tissue-compartment model V_T. Comparisons were performed with repeated-measures ANOVA for V_T values in the various regions, except the cerebellum, using SPSS (version 22

for Windows; SPSS Inc.). The cerebellum was excluded from the ANOVA analysis because it did not reach full stability at 120 min. Variability in binding values was defined as coefficient of variation = SD/mean × 100%. Group data are expressed as mean ± SD, except the kinetic microparameters, which are expressed as median values.

RESULTS

PET Brain Imaging with ^{18}F-FIMX

Pharmacologic Effects. In the 12 subjects who underwent brain scanning and the 4 subjects who underwent whole-body scanning, no adverse events were reported either during or after the scans. In addition, no effects were noted on blood and urine tests, blood pressure, electrocardiogram, or respiratory rate.

Plasma Analysis. Unchanged ^{18}F-FIMX in the arterial plasma peaked at 25 ± 4 SUV about 1.5 min after injection and rapidly declined thereafter (Fig. 1A). Parent radioligand represented 44% ± 7% of radioactivity in plasma at 10 min and 20% ± 6% at 120 min. For the subjects who underwent a longer scan, the parent fraction declined further to reach 11% ± 6% at 210 min. The parent concentration in some blood samples from those who underwent the longer scans (i.e., after 120 min) was higher than that of the preceding sample, suggesting that the parent measurement at later times may be inaccurate. At least 5 radiometabolites were observed (Supplemental Fig. 1), although all appeared less lipophilic than the parent. The f_P was 0.34% ± 0.06% (mean ± SD from 12 subjects).

Brain Images. Brain uptake peaked about 10 min after injection and then rapidly decreased (Fig. 1B). The cerebellum generally peaked later, at about 20 min. Nevertheless, the washout slope from the cerebellum was similar to that from the other regions. Consistent with the known distribution of mGluR1 in the mammalian brain (*23,24*), a high uptake was observed in the cerebellum (SUV_{peak} 4–6), whereas the remaining regions showed intermediate (thalamus) or low concentrations; SUV_{peak} was typically between 2 and 4.

Compartmental Analyses. The brain time–activity curves were better fit by an unconstrained 2-tissue-compartment model than by a 1-tissue-compartment model. The 2-tissue-compartment model had lower mean Akaike information criterion (370) and higher mean model selection criterion (5.1) scores than those for the 1-tissue-compartment model (Akaike information criterion = 431; model selection criterion = 3.2). The superiority of the 2-tissue-compartment model was confirmed by F statistics for all subjects. Moreover, spectral analysis showed at least 2 equilibrating components in each region for all subjects.
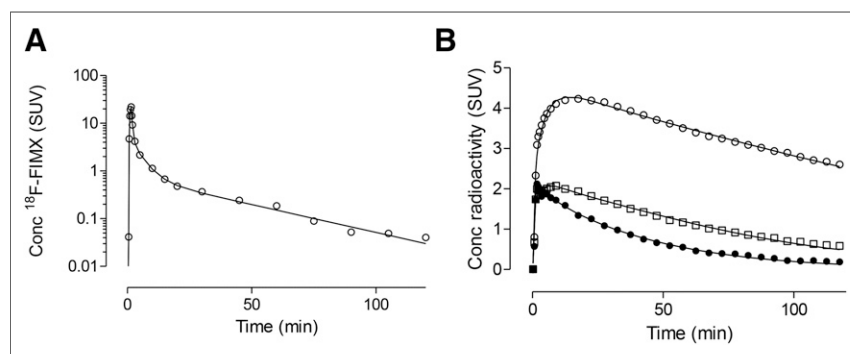
V_T values were stable within the 120-min scan in all regions except the cerebellum (Fig. 2A). For noncerebellar regions, the V_T value at 120 min was about 95% of the value at 210 min (Fig. 2B). In contrast, the cerebellum became relatively stable only later; its V_T values increased slowly (by <5%) only from 170 to 210 min. Two subjects displayed some aberrant V_T values after 120 min (the V_T values were higher at 160–180 min than at 210 min; removing these 2 subjects from the time–stability analysis did not significantly affect the results).

Although the microparameters ($K_1 - k_4$) had only fair identifiability (Supplemental Table 1), the macroparameter V_T was well identified: the SE for the cerebellum was 3.83% and that of the other brain regions was 0.81% on average. Regional V_T values (mL·cm^{-3}) had about a 7-fold range from 1.48 ± 0.17 in the caudate to 11.0 ± 1.9 in the cerebellum (Supplemental Table 2).

The free fraction f_P for ^{18}F-FIMX in plasma was low (0.34% ± 0.06%), and random errors in its measurement may have increased the coefficient of variation (mean/SD × 100%) of V_T/f_P (23%) compared with V_T (13%) in 12 subjects.

Noncompartmental Analyses. All alternative techniques were consistent with a 2-tissue-compartment model at the region level. At the voxel level, the 2 SA techniques yielded poor results (Fig. 3; supplemental data).

Bloodless Quantification. We found that either uptake in each brain region from 50 to 80 min ($SUV_{50–80}$) or ratio in each brain region from 50 to 80 min ($SUVR_{50–80}$) might be used as a bloodless substitute for V_T (supplemental data).

Estimating V_{ND} Using mGluR1 Gene Transcript

To estimate V_{ND} from regional densities of mGluR1 gene transcripts, we sequentially performed 4 analyses: autocorrelation to determine which of the 3 published transcripts was appropriate to use, determination of whether relative gene transcript was proportional to V_T, estimation of V_{ND} from this correlation, and measurement of V_{ND} in monkey brain after complete receptor blockade.

Autocorrelation. The values of each donor tightly correlated with those of any other donor for all 3 transcripts available in the Allen Brain Atlas (Pearson r value ranged from 0.765 to 0.963, all $P < 0.0001$). The mRNA expression values were then averaged among the subjects to obtain the final values for each probe. The autocorrelation between the probes showed a high correlation between probes A and B ($r = 0.897$, $P = 0.0004$), whereas the correlation of probe C to the other 2 was weaker, although still significant ($r = 0.667$, $P = 0.035$, and $r = 0.688$, $P = 0.028$, respectively). Because probe B showed the best correlation with the other 2 probes, it was chosen to perform cross-correlations with PET V_T values. The between-subject autocorrelation for the 2-tissue-compartment model/V_T showed high coefficients ($r > 0.99$), and the V_T values of the 12 subjects were therefore averaged to obtain representative ^{18}F-FIMX V_T values.

Correlation of Gene Transcript and V_T. The mRNA expression values were highly correlated to the mean V_T values ($r = 0.965$, $P < 0.0001$). Notably, this high correlation was predominantly driven by the cerebellum, which is characterized by high mRNA expression and high PET binding. However, the correlation was highly significant even
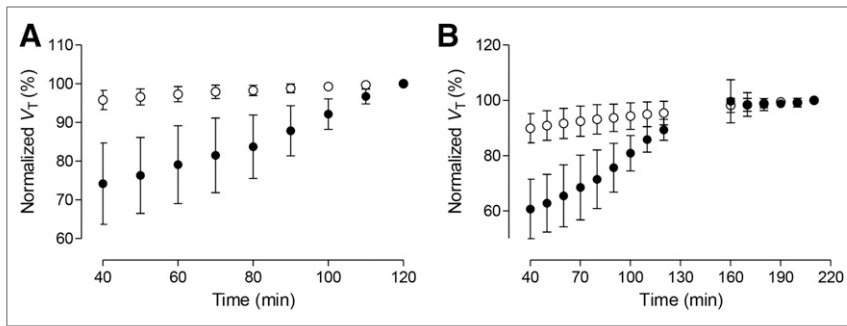

FIGURE 1. (A) Metabolite-corrected arterial input function acquired over 120 min in a representative subject, fitted with a triexponential function. (B) Time–activity curves of brain regions of a subject fitted with 2-tissue-compartment model. Cerebellum (○) had highest uptake, thalamus (□) had intermediate uptake, and caudate nucleus (●) had lowest uptake.

FIGURE 2. Time–stability analysis. V_T results are normalized to 2-tissue-compartment model/V_T values measured at 120 min ($n = 12$) (A) and 210 min ($n = 6$) (B). ● = cerebellum and ○ = average of other brain regions. Although good stability was reached by 120 min in low-uptake regions of brain, cerebellum still showed upward trend at 120 min and eventually almost stabilized by 170 min. Higher SD bars after 160 min denote presence of subjects with aberrant V_T values.

after the cerebellum was excluded from the analysis ($r = 0.823$, $P = 0.0035$). These results suggest that the relative density of gene transcripts can be used as a substitute for V_S in the typical Lassen plot.

Estimating V_{ND} in Human Brain. Following the assumptions of the Lassen plot, the V_{ND} of ^{18}F-FIMX was estimated as the x-intercept of the plot of mGluR1 transcript density versus V_T across brain regions (Fig. 4). That is, when specific binding is absent (x-intercept), the value of V_T equals V_{ND}. By this calculation, V_{ND} was only 0.5 mL·cm^{-3} (Fig. 4), suggesting that most of the total uptake in the brain was specific. For example, in the highest-density region (cerebellum), V_T at 210 min was 13.4 mL·cm^{-3} and V_S was thus 12.9 mL·cm^{-3} (13.4 − 0.5). In the lowest-density region (caudate), V_T was about 1.5 mL·cm^{-3} and V_S was thus 1 mL·cm^{-3} (1.5 − 0.5).

V_{ND}/f_P was similar in human and nonhuman primates (~150 and 170 mL·cm^{-3}, respectively) (supplemental data).

Whole-Body Biodistribution and Dosimetry

The effective dose was 23.4 μSv/MBq on average (supplemental data).

DISCUSSION

This study found that ^{18}F-FIMX is an excellent PET radioligand for imaging and quantifying mGluR1 in the human brain. The distribution of its relatively high brain uptake reflected that of mGluR1. Uptake was quantified as V_T with excellent identifiability using a 2-tissue-compartment model and several other noncompartmental methods. V_T was stable after 120 min of scanning in all regions except the cerebellum (which required 170 min), and this time stability suggests that radiometabolites did not accumulate in the brain. We also report here a novel approach for estimating V_{ND} in the human brain using the relative density of the target gene transcript. This value of V_{ND} in humans was estimated by modifying the Lassen plot and confirmed by a receptor blocking study in monkey. Finally, whole-body scanning showed that radiation exposure from ^{18}F-FIMX was similar to that from other ^{18}F-labeled radioligands.

^{18}F-FIMX appears to be superior to ^{11}C-ITMM, the only other mGluR1 radioligand to provide a signal in the human brain (6). ^{11}C-ITMM had an overall lower brain uptake (1–2.5 SUV) and a slower uptake and washout. In particular, the cerebellum was still in plateau 90 min after ^{11}C-ITMM injection (6). Although time–stability and the identifiability of the parameters (especially V_T and k_4) were not reported in the original paper, it is possible that ^{11}C-ITMM does not allow V_T values to be reliably estimated within the feasible imaging

time for ^{11}C, whose half-life is 20 min. The high density of mGluR1 in the cerebellum may require a longer-lived radionuclide such as ^{18}F; even then, as we found, 170 min were required to obtain time stable V_T values.

Compartmental and Noncompartmental Analyses

^{18}F-FIMX binding was better described by a 2- than a 1-tissue-compartment model, consistent with identification of 2 kinetically distinguishable pools of radioligand—namely, specifically bound and nondisplaceable. V_T (mL·cm^{-3}) values had a 7-fold range, from 1.5 in the caudate to 11 in the cerebellum (Supplemental Table 2). In contrast, the V_T values of ^{11}C-ITMM had only a 3-fold range (from 0.5 to 2.6 mL/cm^3), perhaps reflecting an underestimation and lack of equilibrium in the cerebellum (6).

In theory, V_T values should be corrected by the percentage of radioligand not bound to plasma proteins (V_T/f_P), because only this fraction is available for exchange with the tissues. However, f_P measurement can be an important source of noise, especially when f_P is very low. In this study, the f_P value for ^{18}F-FIMX was quite low (0.34% ± 0.06%), and imprecision in its measurement presumably caused a higher coefficient of variation for V_T/f_P (23%) than for V_T (13.2%) (Supplemental Table 3). This higher variability would require larger sample sizes to detect statistically significant differences between groups.
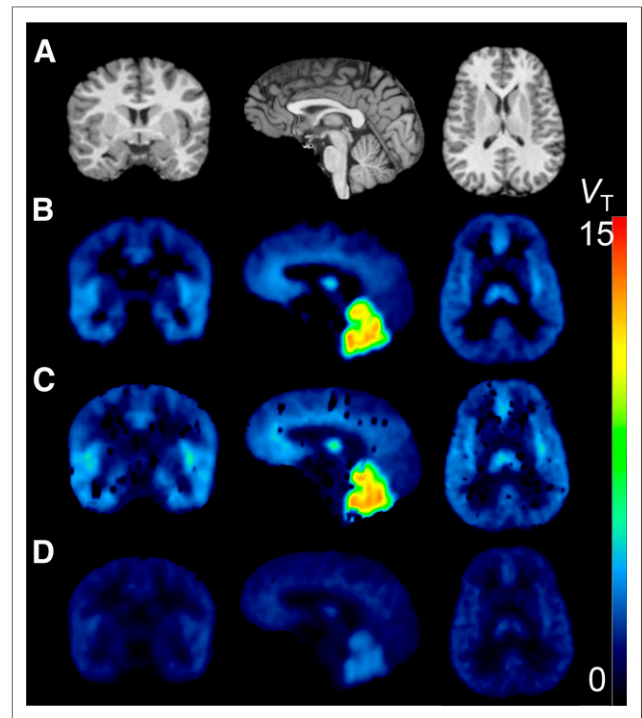

FIGURE 3. Parametric images in a representative subject. (A) MRI. (B) Logan. (C) Standard SA. (D) RSSA. Images obtained with Ichise's multilinear analysis 1 (MA1) and Zhou's RE-GP are visually indistinguishable from Logan images and are not shown. Parametric maps obtained with SA (C) contained many failed voxels randomly scattered across the whole brain. RSSA (D) yielded maps of good quality, but V_T values were severely underestimated compared with 2-tissue-compartment model.
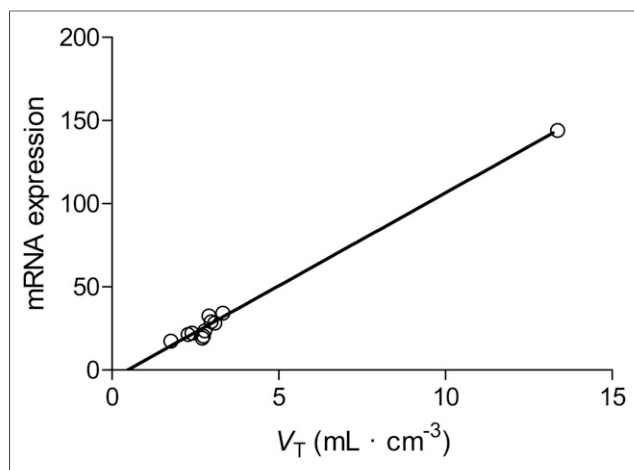
FIGURE 4. Linear regression analysis between mRNA expression values measured by mRNA probe B for mGluR1 gene and average 2-tissue-compartment model/V_T values of ^{18}F-FIMX. V_T of cerebellum, right-most data point, was calculated from 210 min of image acquisition. Linear regression shown in this graph, which includes cerebellum, has R^2 of 0.992 and x-intercept of 0.5 mL·cm^{-3}, which corresponds to V_{ND} of ^{18}F-FIMX. When cerebellum is removed, R^2 becomes 0.648 and x-intercept decreases to 0.3 mL·cm^{-3}.

All noncompartmental techniques provided good and substantially equivalent results at the region level (Supplemental Table 2). Quantification at the voxel level was, however, more challenging. The V_T values obtained with Logan, MA1, and RE-GP were similar to those obtained by the 2-tissue-compartment model at the region level, with an average bias for all regions (excluding the cerebellum) ranging from −6.5% for Logan to −2.1% for RE-GP. Notably, MA1 is known to reduce noise-induced bias of parametric images (15) and, indeed, in the present study yielded a lower bias than Logan (−3.5% vs. –6.5%, $P < 0.05$).

Although SA/V_T values also closely matched 2-tissue-compartment model/V_T (−3% average bias, $P > 0.05$), SA parametric maps contained many outlying voxels randomly scattered across the whole brain, making them unsuitable for statistical parametric comparisons. This finding is not unusual when SA is applied at the voxel level (25). Finally, the maps obtained with RSSA severely underestimated actual V_T values, and this underestimation was region-dependent, for example, greater in the cerebellum (−74%) than other regions (−33%).

Bloodless Methods

This study assessed 3 noninvasive (i.e., bloodless) methods of quantifying ^{18}F-FIMX binding: a reference tissue model (i.e., SRTM), a ratio of brain radioactivity in 1 region compared with another region (i.e., SUVR), and merely the uptake in the region (i.e., SUV). When either the caudate or the cerebellum was used as the reference region, the binding potential relative to the nondisplaceable compartment of SRTM showed higher intersubject variability than V_T (Supplemental Table 3), had poor time stability, and did not even converge in some regions with intermediate density of receptors. The poor performance of SRTM may be due to the fact that no true reference region (i.e., devoid of receptors) exists for mGluR1, and the regions used as reference have a V_T value that is close to that of the other regions. For example, if our estimate of V_{ND} (0.5 mL·cm^{-3}) is accurate, then two thirds of V_T (1.5 mL·cm^{-3}) in the caudate was actually V_S (1.0 mL·cm^{-3}). Whatever the cause of its poor performance, SRTM should not, in our opinion, be used to measure mGluR1 with ^{18}F-FIMX.

In contrast to SRTM, SUVR$_{50-80}$ (using the caudate as a reference region) showed the lowest variability of all techniques (9.9%). SUVR might thus be a practical alternative to full kinetic modeling. However, the use of SUVR in any particular disease will first require confirmation that the sizeable specific binding in caudate does not differ significantly between groups (e.g., patients and controls) or between conditions (e.g., baseline and receptor blocked).

The SUV$_{50-80}$ was well correlated with V_T (Supplemental Fig. 2). SUV$_{50-80}$ is arguably the simplest bloodless method and does not require a reference region or demonstration that the reference region is equivalent between groups.

mGluR1 Gene Transcript to Estimate Specific and V_{ND} of ^{18}F-FIMX

To estimate the specific and nondisplaceable components of ^{18}F-FIMX, we used a version of the Lassen plot, which measures the linear relationship of specific binding as a function of total uptake in the brain. As an overview, the y-axis of the Lassen plot is V_S or a variable proportional to V_S, and the x-axis is V_T or a variable proportional to V_T. In its simplest form (i.e., V_S vs. V_T), when $V_S = 0$, the x-intercept = V_{ND}. That is, when there is no V_S (e.g., in a receptor-free region or after complete receptor blockade), the measured value of V_T will equal V_{ND}. As mentioned, proportional variables can be substituted for V_S or for V_T. For example, Owen et al. (26) showed that V_S can be substituted with 2 variables: V_T baseline minus V_T after partial blockade in numerous brain regions, as the resulting variable is proportional to V_S and the percentage occupancy is the same in all regions when the radioligand occupies a tracer percentage (<5%–10%) of receptors; and for translocator protein radioligands, V_T (high-affinity binders) minus V_T (mixed-affinity binders) is also proportional to V_S and similar across brain regions, as the genetic effect is uniform in brain. In this paper, we introduced the use of transcript density as a substitute for V_S.

This technique has potentially broad applicability, as the Allen Brain Atlas has regional densities for about 30,000 human brain transcripts. However, this technique is applicable only if gene transcript density is linearly proportional to protein density—that is, when the target protein is not subject to significant posttranscriptional changes in vivo. Although this condition was met for ^{18}F-FIMX, this may not always be the case (10). A more extensive validation of the robustness of our modified Lassen plot, in particular by taking human blocked studies as a reference, is under way. By linearly regressing the regional density of mGluR1 gene transcript and V_T, we estimated V_{ND} (i.e., the x-intercept) to be only 0.5 mL·cm^{-3}. Parametric V_T images showed that no region had a consistent number of voxels whose value was about 0.5 mL·cm^{-3}. Likely, all brain regions contain a considerable percentage of specific binding and none would be a pure reference region (according to the Allen Atlas, even white matter expresses a certain amount of mRNA transcript). The accuracy of our V_{ND} estimate was tested against the measured V_{ND} in a nonhuman primate, as the amount of nonspecific binding in the brain is considered to be constant across species (27). Our results showed that V_{ND}/f_P was similar in human and nonhuman primates (about 150 and 170 mL·cm^{-3}, respectively). Notably, when the cerebellum was removed from the analysis and the linear regression was performed only with the remaining regions, the x-intercept decreased from 0.5 to 0.3 mL·cm^{-3}. This suggests a potential limitation of our modified Lassen plot: when the regional V_T values of a radioligand are similar, the V_{ND} obtained can be sensitive to the noise of linear fitting. Therefore, the Lassen plot should preferably be used with radioligands with uneven distributions in the brain.

Dosimetry

According to the pathway we previously proposed for evaluating novel first-in-human ^{18}F-labeled radioligands (*28*), we began the study by obtaining a whole-body scan with a low injected activity (74 MBq) in a healthy volunteer. The aim of this first scan was to verify that the radioligand did not abnormally accumulate in a radiosensitive organ, but it was widely distributed in the body, so that higher activities could be injected for brain imaging. We then proceeded to perform brain imaging by injecting higher activities (~200 MBq) and finally completed the dosimetry part of the study by imaging 3 more subjects with a whole-body scan. The ^{18}F-FIMX effective dose (23.4 μSv/MBq) was similar to the average value of other ^{18}F-labeled ligands (*28*). It could be argued that if a new radioligand shows a typical widespread distribution in the body, the final effective dose is likely to approach the typical average value (*28*). In this case, dosimetry studies might be avoided, and the average value might be used for radioprotection purposes in subsequent clinical studies.

CONCLUSION

^{18}F-FIMX is a new PET radioligand with excellent properties to quantify mGluR1 in the human brain. ^{18}F-FIMX binding was well quantified with both compartmental and noncompartmental methods using a 120-min scan. The high density of mGluR1 in the cerebellum was also accurately quantified, although at least 170 min was required. Regional V_T values of ^{18}F-FIMX were strongly correlated with mGluR1 transcript density, showing that ^{18}F-FIMX uptake was consistent with the expected distribution of mGluR1. Finally, we introduced a modified Lassen plot that uses publicly available data on the regional densities of protein transcripts to estimate specific receptor binding of a radioligand, thereby avoiding the need for receptor blocking studies.

DISCLOSURE

ACKNOWLEDGMENTS

REFERENCES

1. Pike VW. PET radiotracers: crossing the blood-brain barrier and surviving metabolism. *Trends Pharmacol Sci.* 2009;30:431–440.
2. Li S, Huang Y. In vivo imaging of the metabotropic glutamate receptor 1 (mGluR1) with positron emission tomography: recent advance and perspective. *Curr Med Chem.* 2014;21:113–123.
3. Zanotti-Fregonara P, Barth VN, Liow JS, et al. Evaluation in vitro and in animals of a new ^{11}C-labeled PET radioligand for metabotropic glutamate receptors 1 in brain. *Eur J Nucl Med Mol Imaging.* 2013;40:245–253.
4. Zanotti-Fregonara P, Barth VN, Zoghbi SS, et al. ^{11}C-LY2428703, a positron emission tomographic radioligand for the metabotropic glutamate receptor 1, is unsuitable for imaging in monkey and human brains. *EJNMMI Res.* 2013;3:47.
5. Fujinaga M, Yamasaki T, Yui J, et al. Synthesis and evaluation of novel radioligands for positron emission tomography imaging of metabotropic glutamate receptor subtype 1 (mglur1) in rodent brain. *J Med Chem.* 2012;55:2342–2352.
6. Toyohara J, Sakata M, Oda K, et al. Initial human PET studies of metabotropic glutamate receptor type 1 ligand ^{11}C-ITMM. *J Nucl Med.* 2013;54:1302–1307.
7. Satoh A, Nagatomi Y, Hirata Y, et al. Discovery and in vitro and in vivo profiles of 4-fluoro-N-[4-[6-(isopropylamino)pyrimidin-4-yl]-1,3-thiazol-2-yl]-N-methylbenzamide as novel class of an orally active metabotropic glutamate receptor 1 (mGluR1) antagonist. *Bioorg Med Chem Lett.* 2009;19:5464–5468.
8. Xu R, Zanotti-Fregonara P, Zoghbi SS, et al. Synthesis and evaluation in monkey of [^{18}F]4-fluoro-N-methyl-N-(4-(6-(methylamino)pyrimidin-4-yl)thiazol-2-yl) benzamide ([^{18}F]FIMX): a promising radioligand for PET imaging of brain metabotropic glutamate receptor (mGluR1). *J Med Chem.* 2013;56:9146–9155.
9. Cunningham VJ, Rabiner EA, Slifstein M, Laruelle M, Gunn RN. Measuring drug occupancy in the absence of a reference region: the Lassen plot re-visited. *J Cereb Blood Flow Metab.* 2010;30:46–50.
10. Rizzo G, Veronese M, Heckemann RA, et al. The predictive power of brain mRNA mappings for in vivo protein density: a positron emission tomography correlation study. *J Cereb Blood Flow Metab.* 2014;34:827–835.
11. Hawrylycz MJ, Lein ES, Guillozet-Bongaarts AL, et al. An anatomically comprehensive atlas of the adult human brain transcriptome. *Nature.* 2012;489:391–399.
12. Zoghbi SS, Shetty HU, Ichise M, et al. PET imaging of the dopamine transporter with ^{18}F-FECNT: a polar radiometabolite confounds brain radioligand measurements. *J Nucl Med.* 2006;47:520–527.
13. Gandelman MS, Baldwin RM, Zoghbi SS, Zea-Ponce Y, Innis RB. Evaluation of ultrafiltration for the free fraction determination of single photon emission computed tomography (SPECT) tracers: β-CIT, IBF, and iomazenil. *J Pharm Sci.* 1994;83:1014–1019.
14. Logan J, Fowler JS, Volkow ND, et al. Graphical analysis of reversible radioligand binding from time-activity measurements applied to [N-^{11}C-methyl]-(-) cocaine PET studies in human subjects. *J Cereb Blood Flow Metab.* 1990;10:740–747.
15. Ichise M, Toyama H, Innis RB, Carson RE. Strategies to improve neuroreceptor parameter estimation by linear regression analysis. *J Cereb Blood Flow Metab.* 2002;22:1271–1281.
16. Zhou Y, Ye W, Brasic JR, Wong DF. Multi-graphical analysis of dynamic PET. *Neuroimage.* 2010;49:2947–2957.
17. Cunningham VJ, Jones T. Spectral-analysis of dynamic PET studies. *J Cereb Blood Flow Metab.* 1993;13:15–23.
18. Turkheimer FE, Hinz R, Gunn RN, Aston JAD, Gunn SR, Cunningham VJ. Rank-shaping regularization of exponential spectral analysis for application to functional parametric mapping. *Phys Med Biol.* 2003;48:3819–3841.
19. Lassen NA, Bartenstein PA, Lammertsma AA, et al. Benzodiazepine receptor quantification in vivo in humans using [^{11}C]flumazenil and PET: application of the steady-state principle. *J Cereb Blood Flow Metab.* 1995;15:152–165.
20. Hawkins RA, Phelps ME, Huang S-C. Effects of temporal sampling, glucose metabolic rates, and disruptions of the blood-brain barrier on the FDG model with and without a vascular compartment: studies in human brain tumors with PET. *J Cereb Blood Flow Metab.* 1986;6:170–183.
21. Carson RE. Parameter estimation in positron emission tomography. In: Phelps ME, Mazziotta JC, Schelbert HR, eds. *Positron Emission Tomography and Autoradiography: Principles and Applications for the Brain and Heart.* New York, NY: Raven Press; 1986:347–390.
22. Bevington PR, Robinson DK. *Data Reduction and Error Analysis for the Physical Sciences.* New York, NY: McGraw-Hill; 2003.
23. Spooren W, Ballard T, Gasparini F, Amalric M, Mutel V, Schreiber R. Insight into the function of group I and group II metabotropic glutamate (mGlu) receptors: behavioural characterization and implications for the treatment of CNS disorders. *Behav Pharmacol.* 2003;14:257–277.
24. Stephan D, Bon C, Holzwarth JA, Galvan M, Pruss RM. Human metabotropic glutamate receptor 1: mRNA distribution, chromosome localization and functional expression of two splice variants. *Neuropharmacology.* 1996;35:1649–1660.
25. Rizzo G, Veronese M, Zanotti-Fregonara P, Bertoldo A. Voxelwise quantification of [C](R)-rolipram PET data: a comparison between model-based and data-driven methods. *J Cereb Blood Flow Metab.* 2013;33:1032–1040.
26. Owen DR, Guo Q, Kalk NJ, et al. Determination of [^{11}C]PBR28 binding potential in vivo: a first human TSPO blocking study. *J Cereb Blood Flow Metab.* 2014;34:989–994.
27. Di L, Umland JP, Chang G, et al. Species independence in brain tissue binding using brain homogenates. *Drug Metab Dispos.* 2011;39:1270–1277.
28. Zanotti-Fregonara P, Lammertsma AA, Innis RB. Suggested pathway to assess radiation safety of ^{18}F-labeled PET tracers for first-in-human studies. *Eur J Nucl Med Mol Imaging.* 2013;40:1781–1783.